A model for sand waves generation

Paolo BLONDEAUX, Maurizio BROCCHINI and Giovanna VITTORI
D.I.Am., University of Genova, Via Montallegro 1 - 16145 Genova, Italy
Fax: (39)-010-3532546
Email: blx@diam.unige.it - brocchin@diam.unige.it - vittori@diam.unige.it

Abstract

A three-dimensional model for the generation and evolution of sand waves from bottom perturbations of a flat seabed subject to the action of tidal currents and wind waves is proposed. A horizontally-two-dimensional basic flow comprehensive of Coriolis effects, forced by the local climate (tides, residual currents and waves), is considered. Thie flow is completely resolved also in the vertical direction from the free surface down to the seabed. The flow regime is assumed to be turbulent and a Boussinesq's approach based on a space-dependent eddy viscosity is adopted to model Reynolds stresses. Sediment transport is modelled in terms of both suspended load and bed load. The model is capable of predicting the conditions leading to the appearence of sand waves and to determine their main characteristics (wavelength, orientation and migration speed).

Introduction

The bottoms of shallow seas characterized by the presence of tidal currents and large deposits of sand exhibit a variety of regular morphological patterns of different length scales. Among them we find sand waves which are rhythmic features of a few hundred metres in length and heights of a few metres (Stride, 1982). The profile of sand waves is highly symmetric unless either strong residual currents are present or the tidal wave is highly asymmetric. A striking characteristic of sand waves is that they are not static bed forms. Under the action of residual currents they migrate, their crests almost orthogonal to the direction of tide propagation, at a typical rate of about one to some tens of metres per year (Fenster et al., 1990).

Previous studies of the process which leads to the formation of sand waves have shown that these regular features arise as free instabilities of the system describing the interactions between the cohesionless sea bottom and the water motions induced by tide propagation.

Although significant progresses have been made both in the prediction of sand waves appearance and in the prediction of their characteristics (Fredsøe & Deigaard, 1992; De Swart & Hulscher, 1995; Hulscher, 1996) much remains to be done. Indeed to describe the tidal flow, simple hydrodynamic models have been used so far in which important aspects of the phenomenon have been neglected and simple sediment transport predictors have been employed. Moreover, available models fail to give a complete account of some physical effects which are thought of influencing the formation process such as the presence of wind waves, residual currents, suspended load, longitudinal and transverse bed slope effects on the bed load sediment transport.

The aim of the present contribution is to describe the results of a more sophisticated and complete model capable of giving both a more reliable description of the process which leads to the formation of sand waves and more accurate predictions of their characteristics. To this aim the model describes not only the tidal flow but also its interaction with wind waves which often

coexist and can be thought of having a large influence on the growth of bottom forms. Sediments are supposed to move as both bed load and suspended load since field surveys show that large amounts of sediments are put into suspension by the stirring action of sea waves and then transported by tidal currents. Furthermore, residual (steady) currents are taken into account because their presence is essential in explaining sand wave migration. The model is based on the study of the stability of the flat bottom configuration subject to the flow induced by tidal wave propagation. Small bottom perturbations are considered and a linear analysis is performed. Since the morphodynamic time scale is much longer than the hydrodynamic time scale, it is possible to decouple the problem of flow determination from that of analysing the bottom profile evolution. The problem is, thus, reduced to determining the flow field induced by the interaction of the tidal wave with a bottom waviness and then to study the time development of the amplitude of a generic Fourier spatial component of the bottom perturbation which turns out to be periodic in the two horizontal directions.

1 - The model

The model considers a shallow sea of small depth h^* which extends indefinitely in the horizontal directions: the x^*-axis is along the parallels pointing East while the y^*-axis points North along the meridian line. The z^*-axis is vertical pointing upwards. The seabed is supposed to be made of cohesionless sediments of uniform size d^* and density r_s^*. By using the f-plane approximation, the problem of flow determination is posed in terms of continuity and momentum equations for the flow, where Coriolis contribution related to the Earth's rotation (W^* is the angular velocity of the Earth's rotation) is taken into account because it affects tide propagation (hereinafter a star denotes dimensional quantities). The flow regime is assumed to be turbulent and viscous effects are neglected. Moreover, Reynolds stresses are modelled by introducing a kinematic eddy viscosity $n_T^* = n_{T0}^* \, n_T$ (n_{T0}^* being a constant which provides the order of magnitude of the eddy viscosity).

Reynolds equations are made dimensionless on defining the following variables:

where r^* is the sea water density, h_0^* is the local average water depth, w^* is the angular frequency of the tide, U_0^* is the maximum value of the fluid velocity during the tidal cycle. Dimensionless equations depend on four parameters which we denote by s, d , Fr and W respectively:

The parameter s is a kind of Keulegan-Carpenter number and is the ratio between the amplitude of fluid displacement oscillations induced in the horizontal direction by the tidal wave and the local depth. Actual values of s are much larger than one, let us say of order 10^2. The value of d can be thought of as the ratio between the thickness of the viscous bottom boundary layer generated by the tidal wave and the local depth. A rough estimate of d shows that d is a parameter of order one. Fr is the Froude number of the tidal flow which turns out to be smaller than one. Finally, W is the ratio between the angular velocity of the Earth's rotation and the angular frequency of the tidal wave. For a semidiurnal tide W@ 0.5 while for the diurnal tide component W@ 1.

The hydrodynamic problem is then completed by forcing appropriate boundary conditions. At the free surface both a kinematic and a dynamic boundary condition are imposed, the latest forcing the vanishing of the stresses. Because the tidal period is much larger than the turbulence time scale, the flow induced by the tide propagation can be assumed to be slowly varying. Hence, as in steady flows, a boundary condition is specified at the bottom by imposing the vanishing of the velocity at a distance from the seabed equal to a fraction of the roughness z_r^*.

The time development of the bottom configuration is described by the sediment continuity equation:

where $(q_x, q_y) = (q_x^*, q_y^*)/ \ddot{O} (r_s^*/r^*-1)g^*(d^*)^3$ are the dimensionless volumetric sediment transport rates per unit width in the x- and y-directions respectively, s is the Keulegan-Carpenter number already introduced, d is the dimensionless sediment size equal to d^*/h_0^*, $F = U_0^{*2}/(r_s^*/r^*-1) g^* d^*$ is the mobility number of the bottom material and N is the sediment porosity. Equation (2.3) simply relates erosion/deposition processes to spatial increases/decreases of sediment transport. The problem can be closed once a model for the eddy viscosity n_T^* is given and relationships for q_x^* and q_y^* are provided. To this purpose we have adopted an eddy viscosity model similar to that proposed by Van Rijn (1984a,b; 1991) which takes into account the superposition of wind waves to tidal currents. Moreover sediment transport is evaluated following Van Rijn (1984a,b, 1991) and adding a component related to bed slope effects.

More details on both the adopted turbulence model and on the representation of sediment transport contributions can be found in Blondeaux et al. (2000).

2 - The basic flow and the perturbations

The solution of the problem for arbitrary functions h^* is a difficult task. However, in the present analysis small perturbations of the flat bottom configuration are considered. Hence the bottom configuration differs from the flat one of a small amount proportional to e , this being a small (strictly infinitesimal) quantity. The small value of e allows for the solution to be expanded in terms of e .

At the leading order of approximation [i.e. $O(e^0)$], the bottom turns out to be flat and the problem is reduced to the determination of both the flow and sediment transport induced by tide propagation over a flat seabed.

The scaling introduced by (2.1) is appropriate to study the flow induced by the interaction of a tidal wave with bedforms which are characterized by a length scale of the same order of magnitude of the water depth h_0^*. In this case the three velocity components are expected to be of the same order of magnitude. When a tidal wave propagating over a flat bottom is considered, the most appropriate horizontal length scale turns out to be

Moreover, since the ratio h_0^*/L^* is much smaller than one, the horizontal velocity components are much larger than the vertical one. Finally, the vertical displacement a^* of the free surface [i.e. the amplitude of the tidal wave $a^* @ U_0^* h_0^*/(w^*L^*)$] is usually much smaller than the local water depth h_0^* ($a^*/h_0^* \ll 1$). Because of the above considerations, in order to determine the flow induced by tide propagation, it is appropriate to introduce the slow spatial coordinates

and to assume that the basic solution, identified by the subscript '0', can be written in the form

in which 'c.c.' stands for 'complex conjugate', the subscripts label the functions according to the power of e while the superscripts label the functions of the basic flow according to the chosen tidal components (i.e. n=0 refers to residual currents).

Substitution of (3.3) into model equations and into the boundary conditions leads to the equations used to describe the 'basic flow'. Those are used to find the vertical structure of the velocity field for given characteristics of the tidal ellipse (orientation with respect to the x-axis, eccentricity, etc.).

Since the amplitude of the bottom perturbation, the development of which we want to determine, is assumed to be much smaller than the local water depth it is possible to consider a generic spatial component

here e is assumed to be infinitesimal, C (t) is the amplitude of the generic component which is periodic in the x- and y-directions [x=(x,y)] with wavenumbers a_x and a_x respectively [a =(a_x,a_y)]. Because e $\ll$ 1, it is feasible to expand the flow field in the form (only including the semidiurnal tidal component) and the sediment concentration in the form

The factors s and Fr^2 multiplying the perturbations of both the pressure field and of the free surface configuration have been introduced in such a way that p_1 and e_1 are of order one.

When (3.5) is substituted into the flow problem formulated in section 2 and terms of order e^2 are neglected, a set of linear equations for u_1, v_1, w_1, p_1 and e_1 is derived.

A numerical approach, the details of which can be found in Blondeaux et al. (2000), is then used to solve the problem.

The amplitude equation which provides the time development of the amplitude C of the bottom perturbation follows from the sediment continuity equation:

where g is a periodic, complex function of t which depends on the parameters of the problem and is made of four contributions:

The most important contributions are those related to the bed load g_{BC} and to the suspended load g_{SC} due to the tidal currents since the appearance of sand waves and tidal ridges is induced by the propagation of the tidal wave on shallow seas. The value of g is also affected by the wave-related sediment transport g_W but this contribution affects the results only from a quantitative point of view. Finally, the bed slope also affects g providing a contribution g_{slope} which is always real and negative, thus, representing a damping of the perturbations.

The solution of (3.7) is clearly:

Hence, the growth or the decay of the perturbation is controlled by the real part of the time average of g , while the imaginary part is related to the migration speed of the perturbations. The periodic part of g , with vanishing time average, simply describes oscillations of the sand wave configuration around its average configuration.

3 - Discussion of the results

Because of the large number of parameters controlling the behaviour of the system an exhaustive discussion of the results is not possible. Therefore we start by considering a specific set of data which allows for a comparison of the theoretical findings with some field observations. Subsequently, on varying climate parameters, we try to identify the role of the different components involved in the phenomenon of sand waves formation.

We start by considering a location chracterized by a latitude of about 50° North and an average water depth equal to about 20m where sediments of uniform size (d^*=0.45mm) and relative density of 2.65 are present. To make the presentation of the results as simple as possible a first set of model runs has been completed on neglecting the presence of wind waves and on varying the strenght U_0^* of the tidal velocity oscillations while keeping fixed the form of the tidal ellipse (in particular the principal axis of the ellipse is assumed to be parallel to the x-axis and its eccentricity e to be fixed and equal to 0.1) and considering only the semidiurnal component (W @ 0.5). Of course, different values of the parameters induce quantitative variations in the results we are presenting but no qualitative changes. In figure 1 the vertical structure of the basic flow is shown for different values of U_0^* at different phases (5p /16, p /2 and 9p /16) of the tidal cycle. Please notice that the exact symmetry due to tidal flow reversal suggests the same results also characterize phases 21p /16, 3p /2 and 25p /16 respectively. Phases within the cycle have been chosen in such a way that for those values of U_0^* considered in figure 1, the bottom shear stress can mobilize the sediments resting on the bottom. Indeed, for the smallest value of U_0^* (U_0^*=0.60m/s) when 0<t£ 5p /16 and 9p /16£ t<p the Shields parameter is smaller than the critical value. For simplicity only the modulus of the velocity vector is shown on the top panels of figure 1. As it appears from figure 1, the unsteadiness of the flow plays a minor role since the velocity distribution does not significantly differ from the logarithmic law characteristic of a steady current. Also, the sediment concentration distribution is close to that characteristic of steady flows as shown from the bottom panels of figure 1, where the concentration profiles are plotted during the tidal cycle for different values of U_0^*.

In figure 2 the time development of the sediment flow rate (q_x,q_y) is plotted during the tydal cycle for different values of U_0^*. A typical shape, characterized by two symmetric lobes appears. Although there are no reliable measurements of the sediment flux induced by a tidal flow, it is worth to point out that the time behaviour of (q_x,q_y) well agrees with that discussed by Stride (1982).

To show the capability of the model of predicting the appeerence of sand waves the real part g_R of the time average of the function g is obtained as function of a_x and a_y for fixed values of the parameters (related to climate and sediment characteristics). We remind that g_R is the growth rate of the bottom perturbations. Hence, positive values

of g_R imply the growth of the bottom perturbations while negative values of g_R cause the disappearence of any initial bottom disturbance. Finally, when g_R vanishes perturbations neither amplify nor decay. For weak tidal currents (e.g. $U_0^*=0.55$m/s) and the other input parameters as previously defined ($h_0^*=21$m and $d^*=0.45$mm), the bottom shear stress induced by tide propagation is unable to move sediments and, of course, no change in the bottom configuration is induced.

On increasing U_0^* while keeping the other parameters fixed, a critical value $(U_0^*)_c$ is encountered such that for U_0^* larger than $(U_0^*)_c$ sediments start to move and bottom perturbation to develop. Results show that g_R is positive for perturturbation components characterized by wavenumbers falling in a restricted range around a critical value [$(a_x)_c$, $(a_y)_c$] for which the value of g_R is maximum. Hence, the theory suggests that in these conditions perturbations characterized by a dimensionless wavelength equal to about $2p/|a_c|$ will grow and will lead to the appearence of periodic bottom forms. For the water depth and sediment characteristics presently investigated this happens, for example, when $U_0^*=0.60$m/s (see figure 3). Hence, the critical value of U_0^* predicted by the theory falls between 0.55m/s and 0.60m/s in agreement with field observations. Indeed, as described by Stride (1982), sand waves only appear when the amplitude of the tidal velocity oscillations exceeds a threshold of about 0.50-0.55m/s. Moreover, the analysis shows that the bedforms which tend to appear are characterized by crests almost orthogonal to the major axis of the tide since the maximum value of g_R is reached for almost vanishing values of a_y.

This theoretical prediction well agrees with field observations as described for example by Belderson et al. (1982) and Stride (1982). Also the wavelength of sand waves predicted by the theory falls within the range of observed values, since the perturbation component characterized by the maximum amplification rate, i.e. the component which will dominate the bottom configuration, is characterized by $(a_x,a_y) \sim (0.49,-0.10)$ which corresponds to a dimensional wavelength of about 260m, a value in agreement with the size of sand waves observed in the North Sea which range from about 100m to about 500m.

More results on the model validation and performances can be found in Blondeaux et al. (1999, 2000).

References:

Belderson, R.H, Johnson, M.A. and Kenyon, N.H., 1982. Bedforms. In Offshore tidal sands. (ed. A.H. Stride). Chapman & Hall.

Blondeaux, P., Brocchini, M., Drago, M., Iovenitti, L. and Vittori, G., 1999. Sand waves formation: preliminary comparison between theoretical predictions and field data. Proc. IAHR-RCEM Symposium, 1, 197-206.

Blondeaux, P., Brocchini, M. and Vittori, G., 2000. On sand waves and tidal ridges formation: a unified theory. Submitted to J. Fluid Mech.

De Swart, H.E. and Hulscher, S.J.M.H., 1995. Dynamics of large-scale bed forms in coastal seas. In Nonlinear Dynamics and Pattern Formation in the Natural Environment. Eds. A. Doelman & A. Van Harten, Longman, New York.

Fenster, M.S., Fitzgerald, D.M., Bohlen, W.F., Lewis, R.S. and Baldwin, C.T., 1990. Stability of giant sand waves in eastern Long Island Sound, U.S.A., 91, 207-225.

Fredsøe, J. and Deigaard, R., 1992. Mechanics of coastal sediment transport. Advanced Series on Ocean Engineering. World Scientific, Singapore, xviii+369 p.

Hulsher, S.J.M.H., 1996. Tidal-induced large-scale regular bed form patterns in a three-dimensional shallow water model. J. Geophys. Res., C9, 101, 20727-20744.

Stride, A.H., 1982. Offshore tidal sands. Chapman & Hall, London, New York, xi+222 p.

Van Rijn, L.C., 1984a. Sediment transport, part I: bed load transport. J. Hydr. Engng., 110, 1431-1456.

Van Rijn, L.C., 1984b. Sediment transport, part II: suspended load transport. J. Hydr. Engng., 110, 1613--1641.

Van Rijn, L.C., 1991. Sediment transport in combined waves and currents. Proc. Euromech 262, Balkema.
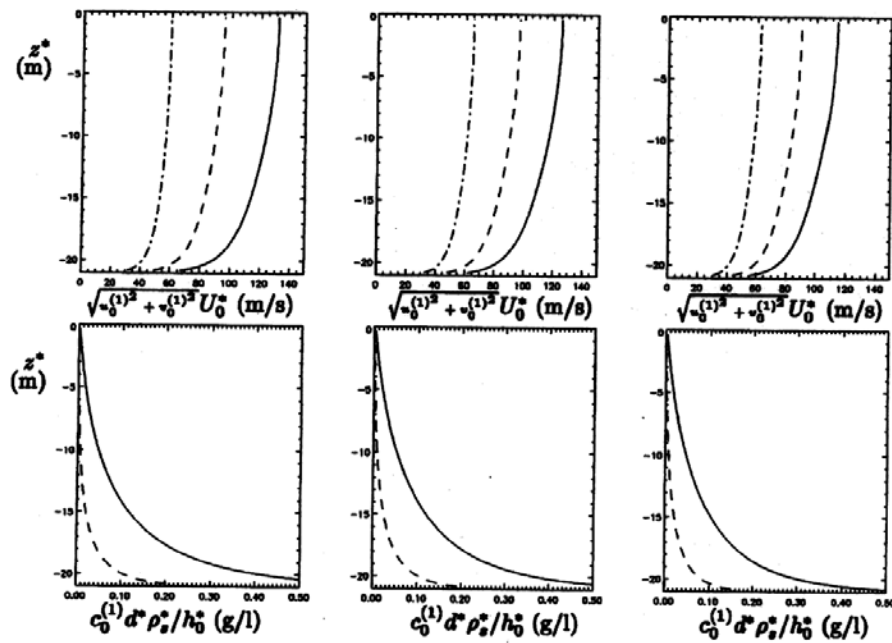
Figure 1 - The vertical structure of the basic flow. Top panels report the profiles of the modulus of the velocity vector for three phases [$5\pi/16$ (left), $\pi/2$ (center) and $9\pi/16$ (right)] of the tidal cycle. Bottom panels report the profiles of sediment concentration at the same phases. Solid lines pertain to profiles obtained with $U_0^* = 1.20$ m/s, while dashed and dotted-dashed lines are related to profiles computed for $U_0^* = 0.90$ m/s and $U_0^* = 0.60$ m/s respectively. For $U_0^* = 0.60$ m/s the concentration of the solid phase is so low that the dotted-dashed line is undistinguishible from the z^*-axis. Other parameters are as described in the text.
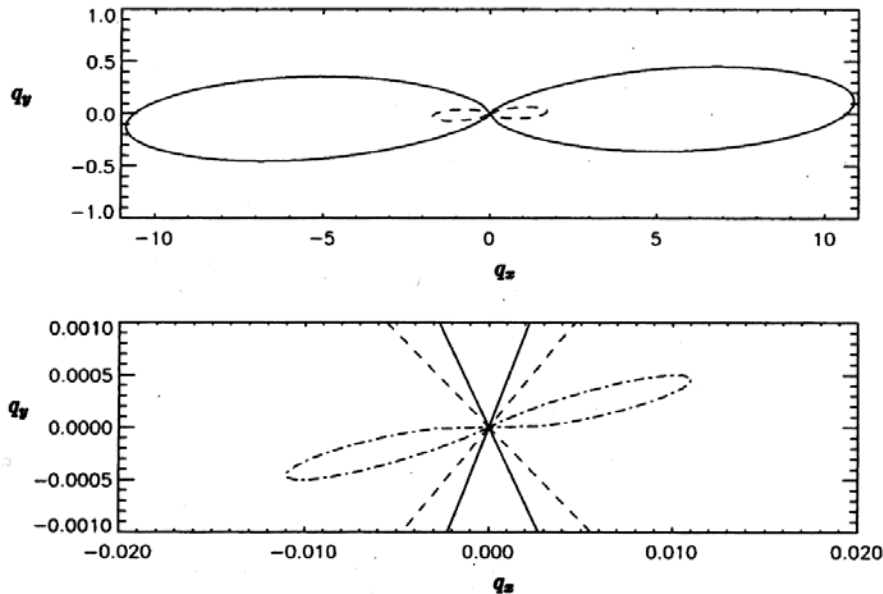

Figure 2 - The horizontal structure of the sediment transport rate during the tidal cycle and for different values of U_0^*. Overview of the (q_x, q_y)-plane. The solid line pertains to the case $U_0^* = 1.20$m/s, while the dashed line is related to $U_0^* = 0.90$m/s.
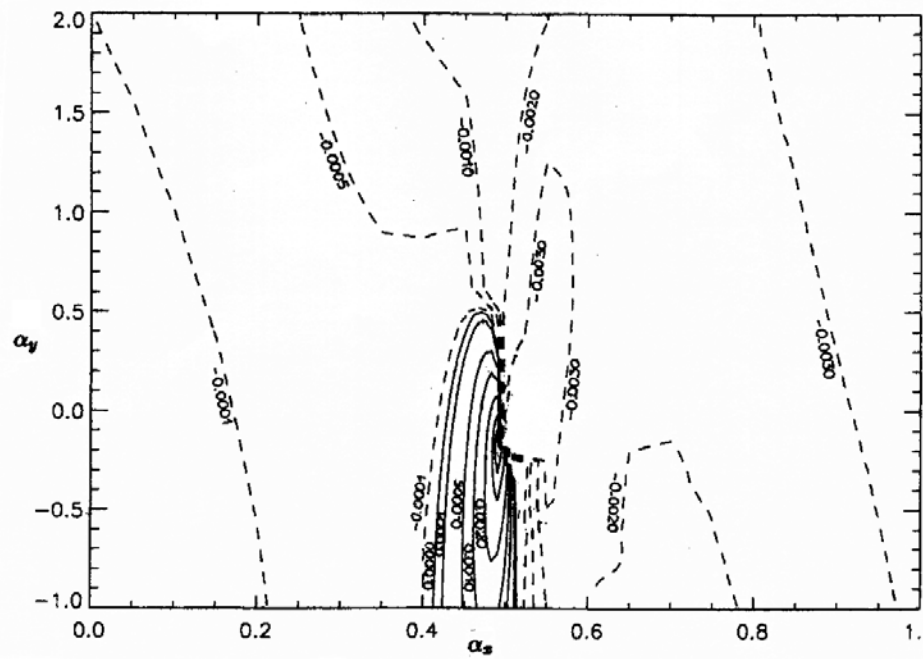
Figure 3 - Beform generation. Contour map of γ_R in the (α_x, α_y)-plane. Case with no wind waves and no residual currents. Input data: $h_0^* = 21$ m, $U_0^* = 0.60$ m/s, $\alpha_C = 0°$, $e = 0.1$ and $d^* = 0.45$ mm. Positive contour lines are drawn in solid while dashed lines pertain to negative values of the growth rate.

Sommaire: